

## Cross-correlation of the Astrophysical Gravitational Wave Background with the Cosmic Microwave Background

G. PERNA<sup>(1)</sup>(<sup>2</sup>)

<sup>(1)</sup> *Dipartimento di Fisica e Astronomia “G. Galilei”, Università degli Studi di Padova  
via Marzolo 8, I-35131 Padova, Italy*

<sup>(2)</sup> *INFN, Sezione di Padova - via Marzolo 8, I-35131 Padova, Italy*

received 31 January 2023

**Summary.** — This article is based on the talk I delivered in “Sezione 3: Astrofisica” of the 108th National Congress of the Italian Physical Society on 12th September 2022. The session was dedicated to Gravitational Waves (GW) and Cosmology. Since the first detection by LIGO/Virgo, GW physics has been very promising, providing a new complementary way to study and understand our Universe. In this work I focused on the analysis and characterization of the Astrophysical Gravitational Wave Background (AGWB) anisotropies, generated at the production and during the propagation of the signal. The physics behind them shows many analogies with the cosmic microwave background ones; thus I focus on the extent they can be used to constrain cosmology, by means of the cross-correlation between the two signals. More specifically, I aim to constrain primordial non-Gaussianity studying its impact on the bias of astrophysical sources of GW. For the purpose, I developed a code to model the astrophysical sources and I modified the code CLASS, implementing the AGWB anisotropies.

### 1. – Introduction

After almost one century since their prediction in 1916 [1, 2], the first Gravitational Wave (GW) has been detected in September 2015 [3]. It has been one of the most important discoveries of the last years and can be considered as a further confirmation of General Relativity (GR). GWs are deemed to be of great importance for the information they can provide about our Universe, both on the astrophysical (*e.g.*, [4]) and on the cosmological sides (*e.g.*, [5, 6]). All the GWs measured up to now share the attribute of being all “resolvable” signals. This means that we have been able to infer the information about the properties of each binary system that generated them, like the masses of the merging compact objects, the distance and location in the sky [7]. One of the challenges of the GW search is the detection and characterization of the Stochastic Gravitational

Wave Background (SGWB) [8-10]. This background is given by the superposition of GW signals that are too numerous or too weak to be individually detected and it is expected to receive a contribution from very recent sources (astrophysical sources like black hole binaries, (BBH), or neutron star binaries, (BNS)) [11-15] and also from the very early Universe (GWs produced during inflation, phase transitions, cosmic strings) [16-18]. This naturally leads to distinguish two different contributions to the background: the former sources generate the Astrophysical Gravitational Wave Background (AGWB), while the latter lead to the Cosmological Gravitational Wave Background (CGWB). We specify that it has not been detected yet, but the latest constraints from the LIGO-Virgo-Kagra (LVK) Collaboration [19,20] and the detection of a possible common red noise process by the NANOGrav Collaboration [21] are promising for an imminent detection in the very next years. Furthermore, for such purpose, future generation interferometers are being planned, like LISA [22], Einstein Telescope (ET) [10] and BBO [23].

In this work we focus on the AGWB. Being a stochastic background it can be characterized only statistically and even though it can provide a lot of population properties about the astrophysical sources that generated it, we study to which extent it can be used to constrain cosmological parameters. The link between the late time evolution of our Universe and its primordial phases resides in the anisotropies of such a background. They can be distinguished in two types, the ones generated at the production of the signal and those produced during its propagation towards the Earth [24-28]. These latter are due to the inhomogeneous and anisotropic structure of our Universe and are related for example to the presence of peculiar velocities of the sources or evolving gravitational potentials in the graviton geodesic, whose presence is strictly linked to the fluctuations of primordial fields. On the other hand the former are due to the intrinsic anisotropic distribution of GW sources in the sky and will be called in the following “density anisotropies”. These ones are at the center of this work since, as we will show in the following, they present a strong dependence on the presence of primordial non-Gaussianity (nG), the observable we are focusing on in our analysis.

Understanding the origin of our Universe —*i.e.*, its primordial phase called inflation [29-31]— is one of the most important aspects of current cosmological searches. A way to distinguish among the huge number of models that have been proposed is the amount of primordial nG [32,33]. In the standard scenario of inflation, the amount of nG is expected to be very small; on the other hand non-standard scenarios allow for a large level of nG (see, *e.g.*, [34]). It clearly follows, that constraining nG would allow us to rule out some of these models. A powerful way to detect primordial nG is the study of the abundance and clustering of rare events: structures in our Universe are generated by the large fluctuations of the primordial density field, expected to lie in the tails of its probability distribution. These tails are affected by the presence of nG and thus the abundance of very rare events is very sensitive to changes in the shape of the distribution, like the ones generated by nG. Typically, the way adopted to study the distribution of the underlying dark matter is the analysis of the structures that we can directly observe from Earth, the tracers (*e.g.*, different types galaxies, GW sources, etc.). Their distribution is related to the underlying matter distribution through the bias and so can be used to infer this latter’s properties.

In this work we focus on the effects of local primordial nG, that result in the presence of an additional scale-dependent correction to the tracers bias, proportional to  $f_{\text{NL}}$ , [35-37]. The statistical tool we adopt in our analysis is the cross-correlation between the AGWB and the Cosmic Microwave Background (CMB). The idea behind this method is related to the presence of some analogies between the anisotropies of the two signals. In our

analysis the cross-correlation arises mainly in the AGWB density anisotropies and the CMB's Integrated Sachs-Wolfe (ISW) effect, as will be explained in the following. We focus on the contribution to the AGWB coming from Black Hole Binaries (BBH) since they are expected to dominate the signal. For such a purpose, we develop a python code to model all the astrophysical dependences of the sources *e.g.*, mass distribution, binary merger rate following the latest constraints coming from the LVK Collaboration [38]. Furthermore we modify the CLASS code [39], including all the anisotropies of the AGWB, the effect of nG on the bias and the astrophysical dependences.

In sect. 2 we discuss the AGWB and its anisotropies, in sect. 3 we briefly discuss about the CMB, while in sect. 4 we discuss quantitatively about the GW bias and the effects of nG. Finally in sects. 5 and 6 we will report our results and conclusions.

## 2. – AGWB characterization

The way to characterize the SGWB is through the GW energy density per logarithmic frequency, defined as

$$(1) \quad \Omega_{\text{GW}}(f_o, \hat{\mathbf{n}}) = \frac{f_o}{\rho_c} \frac{d\rho_{\text{GW}}(f_o, \hat{\mathbf{n}})}{df_o}.$$

We indicated with  $f_o$  the observed frequency and with  $\rho_{\text{GW}}$  and  $\rho_c$ , respectively, the GW energy density and the critical energy density. Note that we also included a dependence on the direction to account also for the anisotropic contribution to  $\Omega_{\text{GW}}$ . Actually the isotropic (also called monopole) and anisotropic contributions can be separated by writing the normalized GW energy density as

$$(2) \quad \begin{aligned} \Omega_{\text{GW}}(f_o, \hat{\mathbf{n}}) &= \bar{\Omega}_{\text{GW}}(f_o) + \Delta\Omega_{\text{GW}}(f_o, \hat{\mathbf{n}}) \\ &= \bar{\Omega}_{\text{GW}}(f_o)(1 + \Delta_{\text{GW}}(f_o, \hat{\mathbf{n}})), \end{aligned}$$

where in the last line we have defined the anisotropic contribution normalized with respect to the monopole,  $\Delta_{\text{GW}}(f_o, \hat{\mathbf{n}})$ . Another differentiation that can be applied to the normalized energy density is related to sources that contribute to it so that one could write

$$(3) \quad \Omega_{\text{GW}}(f_o, \hat{\mathbf{n}}) = \sum_i \Omega_{\text{GW}}^{[i]}(f_o, \hat{\mathbf{n}}),$$

with the index “i” that runs over all the GW sources. In this work we focused only on the contribution coming from black hole binaries, expected to be the dominant one in the astrophysical background.

**2.1. Anisotropic contributions.** – The full calculation of the anisotropies characterizing the AGWB was firstly performed by [28, 40, 41] and by [27] starting from a very general

gauge (see also [42]). We report here the full expression in the Poisson gauge [27]

$$\begin{aligned} \Delta_{\text{GW}}^{[i]}(f_o, \hat{\mathbf{n}}) = & \frac{f_o}{\rho_c} \int \frac{dz}{H(z)} \mathcal{W}^{[i]}(z) \\ & \times \left\{ \delta_{\text{GW}}^{[i]} \right. \\ & + \left( b_{\text{evo}}^{[i]} - 2 - \frac{\mathcal{H}'}{\mathcal{H}^2} \right) \hat{\mathbf{n}} \cdot \mathbf{v} - \frac{1}{\mathcal{H}} \partial_{\parallel} (\hat{\mathbf{n}} \cdot \mathbf{v}) - (b_{\text{evo}}^{[i]} - 3) \mathcal{H}V \\ & + \left( 3 - b_{\text{evo}}^{[i]} + \frac{\mathcal{H}'}{\mathcal{H}^2} \right) \Psi + \frac{1}{\mathcal{H}} \Phi' + \left( 2 - b_{\text{evo}}^{[i]} + \frac{\mathcal{H}'}{\mathcal{H}} \right) \int_0^{\chi(z)} d\chi (\Psi' + \Phi') \\ & \left. + \left( b_{\text{evo}}^{[i]} - 2 - \frac{\mathcal{H}'}{\mathcal{H}^2} \right) \left( \Psi_o - \mathcal{H}_o \int_0^{\eta_o} d\eta \frac{\Psi(\eta)}{1+z(\eta)} \Big|_o - (\hat{\mathbf{n}} \cdot \mathbf{v})_o \right) \right\}. \end{aligned}$$

On the first line in the brace we find the density anisotropies related to the distribution of the GW. Note that here the density is expressed in the synchronous gauge, so it results gauge invariant. It can be related to the underlying matter distribution through the bias as  $\delta_{\text{GW}}^{[i]} = b^{[i]} \delta_m$  [43]. On the second line we find the Kaiser and Doppler terms, related to the peculiar velocity of sources while on the third line we find the gravitational anisotropies due to the presence of gravitational potentials, here indicated with the greek letters  $\Psi$  and  $\Phi$ . The last line reports the terms evaluated at the observer, that contribute only to the monopole and to the dipole, so in this analysis have been neglected. Finally  $H(z)$  is the Hubble parameter and  $\mathcal{W}^{[i]}(z)$  the astrophysical kernel, that we will describe in the next subsection.

**2.2. Astrophysical Kernel.** – The astrophysical kernel is a function that encloses all the astrophysical dependences of the sources considered and can be written as

$$(4) \quad \mathcal{W}^{[i]}(z) \equiv \frac{f_o}{\rho_c} \frac{4\pi}{\bar{\Omega}_{\text{AGWB}}^{[i]}} \frac{w(z, \theta) N^{[i]}(z, f_e, \theta)}{(1+z)}.$$

We model the BBH number density  $N^{[i]}$  following the latest results from the LVK Collaboration<sup>(1)</sup>. Thus we choose the power law plus peak distribution for the masses of the progenitors in the range 4.59–86.22  $M_{\odot}$  and we account for all the sources that merged in the redshift range 0–8 [38]. Furthermore we consider only the contribution coming from unresolved sources by means of a weight function  $w(z, \theta)$ , that accounts only for signals whose SNR does not overcome a certain threshold that we fix to 8 [44]. Finally we model the BBH merger rate as follows. We start from the star formation rate following [45]. Then, since not all the stars end up forming a binary and not all the binaries have merged yet, we multiply the rate by a constant  $\mathcal{A}_1$  that is then fixed by matching it to the BBH merger rate today inferred by LVK [38]. We account for the time delay by weighting the binary merger rate with a time delay probability distribution  $p(t_d) \propto t_d^{-1}$ . We implemented all these astrophysical dependencies in a python code that then we used in combination with the Boltzmann code CLASS to obtain the cross-correlation signal.

---

<sup>(1)</sup> Note that in eq. (4)  $f_e$  is the frequency at the emission of the signal, while  $\theta$  represents the astrophysical parameters we consider.

**2.3. Angular decomposition.** – We conclude the AGWB analysis by projecting the anisotropies on the sphere using the spherical harmonics. It leads to<sup>(2)</sup>

$$(5) \quad \Delta_{\text{GW}}(f_o, \hat{\mathbf{n}}) = \sum_{\ell m} a_{\ell m}^{\text{AGWB}}(f_o) Y_{\ell m}(\hat{\mathbf{n}}).$$

Here the  $a_{\ell m}^{\text{AGWB}}(f_o)$ 's are the coefficients of the expansion and contain all the information about the anisotropies. Actually they are proportional to the primordial curvature perturbation and so they are stochastic variables. Thus we characterize them using the angular 2-point correlation function so that one can write

$$(6) \quad \left\langle a_{\ell m}^{\text{AGWB}*} a_{\ell' m'}^{\text{AGWB}} \right\rangle = \delta_{\ell \ell'} \delta_{m m'} C_{\ell}^{\text{AGWB}}.$$

In the last expression the  $C_{\ell}^{\text{AGWB}}$  indicates the auto-correlation angular power spectrum.

### 3. – CMB

The other observable we consider in our work in order to build the cross-correlation is the CMB. For the purpose of this article we will just report a brief introduction mainly focusing on its anisotropies (*e.g.*, see [46]). The CMB is made of photons that decoupled from the rest of the Universe almost at redshift  $z \sim 1100$  and then propagated freely, reaching us after being redshifted due to the expansion of the Universe itself. As anticipated before, also this signal presents some anisotropies imprinted during the propagation of the signal: the Sachs-Wolfe (SW) effect, the Doppler and the ISW. The first one is related to the gravitational redshift of the photons while coming out of the potential wells at the moment of the decoupling. The second effect is mainly due to relative motion of the photons fluid with respect to the observer. Finally the ISW is still a gravitational effect, but with a different explanation. It is related to the evolution in time of the gravitational potentials during the various epochs (early matter domination and dark energy domination) that affects the propagation of the CMB photons. Thus one can distinguish two different contributions to this effect, an early one due to the fact that at the decoupling the Universe was not in full matter domination (during which the potentials do not evolve and so this effect is vanishing) and a late one, effective since the Universe entered in the dark energy epoch. Starting from the photons Boltzmann equation it is possible to obtain an expression for such anisotropic contributions that can be decomposed on the sphere, yielding

$$(7) \quad \left\langle a_{\ell m}^{\text{CMB}*} a_{\ell' m'}^{\text{CMB}} \right\rangle = \delta_{\ell \ell'} \delta_{m m'} C_{\ell}^{\text{CMB}}.$$

### 4. – Primordial nG and bias

In this section we will finally report the effects of primordial nG on the bias in a more quantitative fashion. Many models of nG have been proposed and can be grouped depending on the shape of the bi-spectrum they generate (see *e.g.*, [34,47] and references

---

<sup>(2)</sup> We specify that in eq. (5) we change the label of the coefficients  $a_{\ell m}$  from GW to AGWB since we focus in this work only on the AGWB contribution, even though the expression is completely general.

therein). Among these we consider the effects of the local-shape on the bias. In this case the Bardeen nG potential  $\Phi$  can be written using an auxiliary Gaussian potential  $\phi$  as [48, 49]

$$(8) \quad \Phi(\mathbf{x}) = \phi(\mathbf{x}) + f_{\text{NL}} (\phi^2(\mathbf{x}) - \langle \phi^2(\mathbf{x}) \rangle).$$

Here we introduced the  $f_{\text{NL}}$  parameter that is used to quantify the amount of nG. The authors of [35-37] showed that starting from this parametrization it is possible to obtain a scale-dependent correction to the bias

$$(9) \quad \Delta b(z, k) = 3f_{\text{NL}}(b-1)\delta_c \frac{\Omega_m}{T(k)D(z)k^2} \left( \frac{H_0}{c} \right)^2.$$

In the last expression  $T(k)$  is the matter transfer function,  $D(z)$  the growth function,  $H_0$  the Hubble parameter today and  $c$  the speed of light. Here  $\delta_c$  is a threshold coming from spherical collapse models and  $b$  is the bias defined in sect. 2.1. We underline the dependence of such correction on the factor  $f_{\text{NL}}/k^2$ . The proportionality to  $f_{\text{NL}}$  suggests the dependence of this correction, from now on called “nG correction”, on the amount of nG predicted by a particular model, while the dependence on the inverse square of the wave-number  $k$  indicates that the correction will be more relevant on the largest scales, where  $k$  is very small.

## 5. – Results

After this introduction we finally report the cross-correlation power-spectrum we obtained. We cross-correlated the AGWB anisotropies with the CMB ones, including the effects of local primordial nG on the bias of GW sources. We modified the public code CLASS [39] to obtain the cross-correlation power spectrum, including all the AGWB anisotropic terms and the nG contribution. We also included the effects due to the astrophysical kernel obtained developing an external python module and that behaves as a window function in redshift, as one can see from eqs. (4) and (10). We report the results

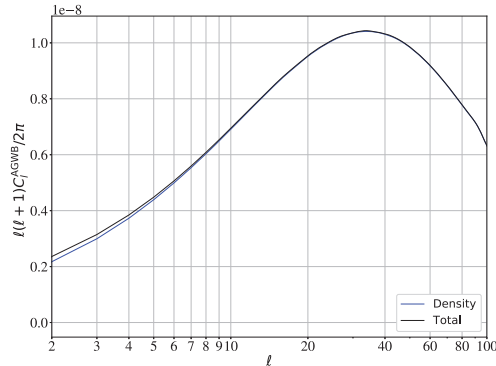


Fig. 1. – The plot shows the cross-correlation angular power spectrum of the AGWB with the CMB. We report the total cross-correlation signal (black line) and the cross-correlation between the density anisotropies and the late-ISW (blue line). This latter, as expected, dominates the signal, almost coinciding on all scales with the total signal.

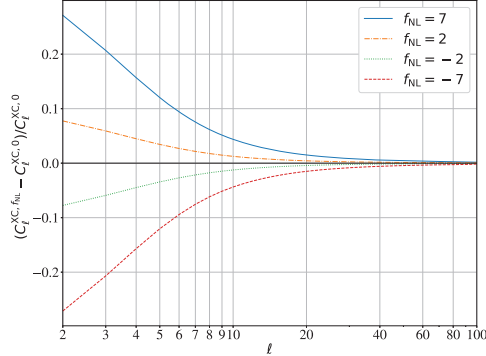


Fig. 2. – The plot shows the percentage difference of the angular power spectrum for the cross-correlation between the AGWB and the CMB of the nG cases with respect to the Gaussian one for different values of  $f_{\text{NL}}$ . We show that the nG contribution leads to a suppression (or enhancement) up to the  $\sim 30\%$  on large scales. The exact behaviour of the curves is actually dependent on the clustering properties of the GW sources, *i.e.*, on the parameters  $b$  and  $p$  considered.

obtained in fig. 1. As the plot shows, the dominant contribution comes from the cross-correlation of the CMB (mainly in the ISW effect) with the density anisotropies. Actually this behaviour was expected and can be explained as follows. The ISW effect, if we now consider its late contribution, is mainly due to the decay of the gravitational potentials on large scales that happens very recently in time. On the other hand, matter in the Universe traces these underlying gravitational potentials and the matter distribution is traced by the GW sources we consider. Therefore a non-zero spatial correlation between the CMB and the AGWB is expected and the ISW-density anisotropies term has to dominate it. Furthermore the behaviour of the whole signal can be explained by considering mainly just this contribution: the late-ISW shows a decreasing behaviour as the scale decreases ( $\ell$  increases) while the density anisotropies show a growing behaviour as one moves to small scales. It is reasonable that the cross-correlation among the two has to grow on large scales, reach a peak and then decrease when the ISW vanishing behaviour starts to dominate. We now report as an example the explicit expression for the  $C_\ell$  related to the dominant contribution accounting also for the nG contribution to the bias. One obtains

$$\begin{aligned}
 C_\ell^{\text{ISW} \times \delta_m} &= \frac{2}{\pi} \sum_{[i]} \int dk k^2 P_\zeta(k) \int_0^{\eta_0} d\eta [T'_\Psi(\eta, k) + T'_\Phi(\eta, k)] e^{-\tau} j_\ell(k(\eta_0 - \eta)) \\
 &\times \int_0^{\eta_0} d\eta \mathcal{W}^{[i]}(\eta) \left[ b^{[i]} + 3f_{\text{NL}}(b^{[i]} - 1) \delta_c \frac{\Omega_m}{T(k)D(\eta)k^2} \left( \frac{H_0}{c} \right)^2 \right] \\
 &\times j_\ell(k(\eta_0 - \eta)) T_\delta(\eta, k).
 \end{aligned}$$

In this equation,  $T_\phi$ ,  $T_\psi$  and  $T_\delta$  are transfer functions, linking the gravitational potentials  $\Phi$  and  $\Psi$  and the density contrast  $\delta$  to the primordial curvature perturbation  $\zeta$ , whose power spectrum (*i.e.*, the two-point correlation function in Fourier space) is  $P_\zeta(k)$ . The  $j_\ell$ 's are the spherical Bessel functions and  $\eta$  is the conformal time. The effects of nG on the cross-correlation as also shown in fig. 2 are more relevant on large scales and result in a suppression or enhancement of the spectrum on those scales. More precisely fig. 2 reports the percentage difference of the nG spectrum with respect to the Gaussian one. We consider different amounts of nG in the range  $-7 \leq f_{\text{NL}} \leq 7$ . The amplitude of

the spectrum varies up to  $\sim 30\%$  on large scales and this could make the difference in the detection of the signal. We also underline that the current, but also future planned detectors are expected to be more sensitive to the largest scales, so it is clear the importance of understanding the behaviour of the spectrum on the smallest  $\ell$ s. It is dutiful also to underline that the symmetry in the enhancements/suppressions of the spectrum is due to the linear dependence on  $f_{\text{NL}}$  of the cross-correlation, as shown in eq. (10). The same behavior, for example, is not present when considering the auto-correlation signal in which the dependence on  $f_{\text{NL}}$  presents both a linear and a quadratic term, leading to asymmetric effects on the angular power spectrum.

## 6. – Conclusion

We considered the cross-correlation of the AGWB with the CMB considering the effects of primordial nG on the bias. We used the well-studied characterization of the CMB anisotropies and the characterization of the AGWB ones following [46] and [27], respectively. Moreover, we accounted for the effects of primordial nG on the bias as firstly shown by [35-37]. In this work we explored the possibility of using GW sources contributing to the AGWB as tracers of the underlying dark matter distribution and the extent this signal can be used to constrain nG. We introduced the theoretical formalism of the CMB and AGWB anisotropies and then we discussed the cross-correlation signal. This latter is expected to be mainly given by the correlation between the density anisotropies and the (late)-ISW effect, both being very recent and important on large scales. We confirmed such a behaviour by plotting the expected angular power spectrum obtained modifying the publicly available code CLASS. We added the effects of local primordial nG on the bias and the AGWB anisotropies. Furthermore, we developed a python code to model the population of BBH considered, accounting for the latest results coming from LVK collaboration. We verified that the inclusion of primordial nG would lead an enhancement (or a suppression) of the power spectrum up to  $\sim 30\%$  for the values of  $f_{\text{NL}}$  we considered with respect to the absence of such corrections on large scales.

\* \* \*

The author acknowledges Angelo Ricciardone, Daniele Bertacca and Sabino Matarrese for the effort, the support and the contribution they provided in developing this work.

## REFERENCES

- [1] EINSTEIN A., *Sitzungsber. Preuss. Akad. Wiss. Berlin (Math. Phys.)*, **1915** (1915) 844.
- [2] EINSTEIN A., *Sitzungsber. Preuss. Akad. Wiss. Berlin (Math. Phys.)*, **1916** (1916) 688.
- [3] ABBOTT B. *et al.*, *Phys. Rev. Lett.*, **116** (2016) 061102.
- [4] VAN DEN BROECK C., *J. Phys.: Conf. Ser.*, **484** (2014) 012008.
- [5] SATHYAPRAKASH B. and SCHUTZ B., *Living Rev. Relativ.*, **12** (2009) 2.
- [6] ABBOTT B. *et al.*, *Nature*, **551** (2017) 85.
- [7] <https://www.ligo.org/detections.php>.
- [8] SATHYAPRAKASH B. *et al.*, “Scientific Potential of Einstein Telescope”, in *46th Rencontres De Moriond On Gravitational Waves and Experimental Gravity*, 2011, pp. 127–136.
- [9] ABBOTT B. *et al.*, *Class. Quantum Grav.*, **34** (044001) 2017.
- [10] MAGGIORE M. *et al.*, *JCAP*, **3** (2020) 050.
- [11] FERRARI V., MATARRESE S. and SCHNEIDER R., *Mon. Not. R. Astron. Soc.*, **303** (1999) 258.

- [12] IGNATIEV V., KURANOV A., POSTNOV K. and PROKHOROV M., *Mon. Not. R. Astron. Soc.*, **327** (2001) 531.
- [13] HOWELL E., COWARD D., BURMAN R., BLAIR D. and GILMORE J., *Mon. Not. R. Astron. Soc.*, **351** (2004) 1237.
- [14] REGIMBAU T. and CHAUVINEAU B., *Class. Quantum Grav.*, **24** (2007) S627.
- [15] REGIMBAU T., *Res. Astron. Astrophys.*, **11** (2011) 369.
- [16] BARTOLO N. *et al.*, *JCAP*, **12** (2016) 026.
- [17] GUZZETTI M., BARTOLO N., LIGUORI M. and MATARRESE S., *Riv. Nuovo Cimento*, **39** (2016) 399.
- [18] CAPRINI C. and FIGUEROA D., *Class. Quantum Grav.*, **35** (2018) 163001.
- [19] ABBOTT R. *et al.*, *Phys. Rev. D*, **104** (2021) 022004.
- [20] ABBOTT R. *et al.*, *Phys. Rev. D*, **104** (2021) 022005.
- [21] ARZOUMANIAN Z. *et al.*, *Astrophys. J. Lett.*, **905** (2020) L34.
- [22] AMARO-SEOANE P. *et al.*, *Laser Interferometer Space Antenna*, arXiv:1702.00786 [astro-ph.IM] (2017).
- [23] CORBIN V. and CORNISH N., *Class. Quantum Grav.*, **23** (2006) 2435.
- [24] CONTALDI C., *Phys. Lett. B*, **771** (2017) 9.
- [25] BARTOLO N., BERTACCA D., MATARRESE S., PELOSO M., RICCIARDONE A., RIOTTO A. and TASINATO G., *Phys. Rev. D*, **100** (2019) 121501.
- [26] BARTOLO N., BERTACCA D., MATARRESE S., PELOSO M., RICCIARDONE A., RIOTTO A. and TASINATO G., *Phys. Rev. D*, **102** (2020) 023527.
- [27] BERTACCA D., RICCIARDONE A., BELLOMO N., JENKINS A., MATARRESE S., RACCANELLI A., REGIMBAU T. and SAKELLARIADOU M., *Phys. Rev. D*, **101** (2020) 103513.
- [28] CUSIN G., DVORKIN I., PITROU C. and UZAN J., *Mon. Not. R. Astron. Soc.*, **493** (2020) L1.
- [29] STAROBINSKII A., *Zh. Eksp. Teor. Fiz. Pis'ma Red.*, **30** (1979) 719.
- [30] GUTH A., *Phys. Rev. D*, **23** (347) 1981
- [31] LINDE A., *Phys. Lett. B*, **108** (1982) 389.
- [32] LUCCHIN F. and MATARRESE S., *Astrophys. J.*, **330** (1988) 535.
- [33] MATARRESE S., VERDE L. and JIMENEZ R., *Astrophys. J.*, **541** (2000) 10.
- [34] BARTOLO N., KOMATSU E., MATARRESE S. and RIOTTO A., *Phys. Rep.*, **402** (2004) 103.
- [35] DALAL N., DORE O., HUTERER D. and SHIROKOV A., *Phys. Rev. D*, **77** (2008) 123514.
- [36] MATARRESE S. and VERDE L., *Astrophys. J. Lett.*, **677** (2008) L77.
- [37] SLOSAR A., HIRATA C., SELJAK U., HO S. and PADMANABHAN N., *JCAP*, **8** (2008) 031.
- [38] THE LIGO SCIENTIFIC COLLABORATION, THE VIRGO COLLABORATION and THE KAGRA COLLABORATION, *The population of merging compact binaries inferred using gravitational waves through GWTC-3*, arXiv e-prints, arXiv:2111.03634 (2021).
- [39] LESGOURGUES J., *The Cosmic Linear Anisotropy Solving System (CLASS) I: Overview*, arXiv e-prints, arXiv:1104.2932 (2011).
- [40] CUSIN G., PITROU C. and UZAN J., *Phys. Rev. D*, **96** (2017) 103019; **493** (2020) L1.
- [41] JENKINS A., SAKELLARIADOU M., REGIMBAU T. and SLEZAK E., *Phys. Rev. D*, **98** (2018) 063501.
- [42] BELLOMO N., BERTACCA D., JENKINS A., MATARRESE S., RACCANELLI A., REGIMBAU T., RICCIARDONE A. and SAKELLARIADOU M., *JCAP*, **06** (2022) 030.
- [43] JEONG D., SCHMIDT F. and HIRATA C., *Phys. Rev. D*, **85** (2012) 023504.
- [44] KARNESIS N., BABAK S., PIERONI M., CORNISH N. and LITTENBERG T., *Phys. Rev. D*, **104** (2021) 043019.
- [45] MADAU P. and DICKINSON M., *Annu. Rev. Astron. Astrophys.*, **52** (2014) 415.
- [46] HU W., *Wandering in the Background: a Cosmic Microwave Background Explorer* (University of California, Berkeley) 1995.
- [47] LIGUORI M., SEFUSATTI E., FERGUSSON J. and SHELLARD E., *Adv. Astron.*, **2010** (2010) 980523.
- [48] GANGUI A., LUCCHIN F., MATARRESE S. and MOLLERACH S., *Astrophys. J.*, **430** (1994) 447.
- [49] KOMATSU E. and SPERGEL D., *Phys. Rev. D*, **63** (063002) 2001.